Unsaturated Hydraulic Conductivity from Transient Multistep Outflow and Soil Water Pressure Data

S. O. Eching, J. W. Hopmans,* and O. Wendroth

ABSTRACT

Soil water retention and unsaturated hydraulic conductivity functions [$K(\theta)$] estimated by the inverse solution technique through minimization of differences between measured and simulated transient outflow may be nonunique and differ from independently measured soil hydraulic data. Numerical and experimental studies have shown the benefit of using simultaneously measured soil water pressure head in the estimation of the soil water retention curve by the inverse technique. In this experimental study, soil water pressure head and transient cumulative outflow measured simultaneously are used to estimate $K(\theta)$. An alternative method for the direct measurement of $K(\theta)$ from transient multistep outflow experiments was adopted. Desorption experiments were carried out for disturbed Yolo silt loam (fine-silty, mixed, nonacid, thermic Typic Xerorthent), Panoche loam (fine-loamy, mixed [calcareous], thermic Typic Torriorthent), Hanford sandy loam (coarse-loamy, mixed, nonacid, thermic Typic Xerorthent), and Oso Flaco fine sand columns. The optimized $K(\theta)$ values agreed well with the directly measured data for all soils, except the sand. Additionally, soil hydraulic functions so obtained for the Panoche loam agreed well with those determined using the evaporation method. Measured infiltration in a column of the Panoche loam matched numerical results using optimized parameters as determined from a sorption multistep experiment. The addition of soil water pressure head values in the optimization procedure provides unique parameters for the unsaturated hydraulic conductivity functions under our experimental conditions.

NUMERICAL MODELS are extensively used in the modeling of water and solute transport in unsaturated porous media. The application of these models depends on knowledge of the soil hydraulic conductivity, K, as a function of water content, θ, or soil water pressure head, h, and the soil water retention function, $\theta(h)$. With the interest in soil spatial variability, there is an increasing need for techniques to determine these functions fast and accurately. Over the years, numerous in situ and laboratory methods have been developed to determine these soil hydraulic properties. Although in situ methods generate results that are more representative of field conditions, laboratory experiments offer more flexibility in initial and boundary conditions. Soil hydraulic functions are also more accurately and more conveniently measured in the laboratory, and measurements are made faster across a wider range of soil water content. Consequently, research has been directed toward developing direct and indirect laboratory methods.

A variety of direct methods have been developed to determine unsaturated hydraulic conductivity data under steady-state conditions (Nielsen et al., 1960; Watson, 1967; Klute and Dirksen, 1986). These methods are time consuming since experiments have to reach several steady-state conditions. Faster non-steady- and quasi-steady-state methods include the hot-air method (Arya et al., 1975), sorptivity method (Dirksen, 1979), the method of Ahuja and El-Swaify (1976), and several evaporation methods (Wind, 1968; Flocker et al., 1968; Plagge et al., 1990). Recently, Wendroth et al. (1993), reevaluated the evaporation method.

In the past, indirect methods have relied on statistical pore-size distribution models to predict the hydraulic conductivity from soil water retention data (Childs and Collis-George, 1950; Burdine, 1953; Mualem, 1976). In recent years, however, the inverse solution technique applied to laboratory outflow data has become an attractive alternative for the indirect estimation of unsaturated hydraulic conductivity data. Outflow experiments are flexible in initial and boundary conditions, yield fast results across a wide range of water content, and are relatively cheap. The technique involves analytical (Gardner, 1956) or numerical solution of the Richards equation subject to imposed initial and boundary conditions. A transient-flow experiment is carried out on a saturated or near-saturated soil core with known initial and boundary conditions. Drainage is induced in one step (Kool et al., 1985) or by multistep (van Dam et al., 1990; Eching and Hopmans, 1993) pressure increments. These transient experiments are faster than steady-state experiments. For the numerical solution, the flow process is subsequently simulated using parameterized hydraulic functions. The unknown parameters are estimated by minimizing deviations between observed and predicted flow variables in the objective function (Dane and Hruska, 1983; Kool et al., 1985; Yeh, 1986; Kool et al., 1987; Kool and Parker, 1988; Eching and Hopmans, 1993). Laboratory outflow experiments used thus far have involved use of transient cumulative outflow supplemented with a limited number of soil water pressure head or soil water content data. However, problems have been reported on the nonuniqueness of the solution (Russo et al., 1991; Toorman et al., 1992; van Dam et al., 1992).

Although the benefit of using soil water pressure data in combination with water content data derived from cumulative outflow is clear from theory (Kool and Parker, 1988; Toorman et al., 1992), few laboratory studies have been reported in the literature. Eching and Hopmans (1993) confirmed the theoretical analysis of Toorman et al. (1992) and showed the improvement in the estimation of $\theta(h)$ from various one-step and multistep outflow experiments if cumulative outflow is combined with simultaneously measured soil water pressure head data. This study determined unsaturated hydraulic conductivity functions estimated by the inverse solution technique with cumulative outflow and soil water pressure head

S.O. Eching and J.W. Hopmans, Hydrologic Science, Dep. of Land, Air, and Water Resources, Veihmeyer Hall, Univ. of California, Davis, CA 95616; and O. Wendroth, Institut für Bodenforschung Zentrum für Agrarlandschafts-und Landnutzungsforshung, Wilhelm-Pieck-straße 72, 0-1278 Müncheberg, Germany. Received 19 Mar. 1993. *Corresponding author (jwhopmans@ucdavis.edu).

Published in Soil Sci. Soc. Am. J. 58:687-695 (1994).

measured simultaneously during laboratory transient multistep outflow experiments. We compared results obtained by computer optimization using the inverse technique with results from our direct measurement technique based on the method of Ahuja and El-Swaify (1976). Moreover, results of the Panoche soil were compared with results from the evaporation method (Wendroth et al., 1993). Additionally, an infiltration experiment was conducted on the Panoche soil. Results for the infiltration experiment were compared with results obtained from a one-dimensional numerical simulation model, using soil hydraulic functions from a multistep sorption experiment as model inputs. Finally, we examined the uniqueness of the optimized parameters.

MATERIALS AND METHODS

Multistep Outflow

The calculation of $K(\theta)$ using the inverse solution technique uses the combination of van Genuchten's $\theta(h)$ model (1980)

$$\Theta = [1+|\alpha h|^n]^{-m} \quad [1]$$

$$\Theta = \frac{\theta - \theta_r}{\theta_s - \theta_r} \quad [2]$$

with the pore-size distribution model of Mualem (1976) to yield (van Genuchten, 1980)

$$K(\theta) = K_s \Theta^l [1-(1-\Theta^{1/m})^m]^2 \quad [3]$$

where Θ is the effective saturation ($0 \leq \Theta \leq 1$), θ_r ($m^3\ m^{-3}$) and θ_s ($m^3\ m^{-3}$) are the residual and saturated water contents, respectively; K_s (cm h^{-1}) is the saturated hydraulic conductivity; α (cm^{-1}), n, m ($m = 1 - 1/n$), and l (assumed to be = 0.5) are empirical parameters. In order to simulate outflow and pressure head in the optimization of the parameters of the hydraulic model, we modified the program MULSTP (van Dam et al., 1990), which is based on ONESTEP (Kool et al., 1985).

The analyses in this study pertain to the same experiments described by Eching and Hopmans (1993). The experimental setup consisted of a 6-cm soil column in a Tempe pressure cell modified to accommodate a microtensiometer–transducer system (Fig. 1), and a 0.57-cm-thick, 1000-cm air-entry ceramic (porous) plate at the bottom. A tensiometer was installed vertically with the cup centered 3 cm below the soil column surface. Soil samples were sieved and packed to predetermined bulk densities. Soil texture and bulk densities are shown in Table 1. Soil samples were saturated from the bottom and subsequently equilibrated to an initial soil water pressure head of −30 cm at the column center. Multistep pressurized outflow experiments were performed on the four soils using N_2 gas in a constant-temperature room at 20°C. Pressure was applied through Port P (Fig. 1) in steps to values of 40, 60, 80, 200, 400, and 700 cm pressure head for the Yolo silt loam; 40, 60, 80, 100, 200, 400, and 700 cm for the Panoche loam and the Hanford sandy loam; and 40, 60, 80, and 200 cm for the Oso Flaco fine sand.

In addition to the above experiments, a multistep experiment to pressure head values of 30, 60, 80, 100, 200, and 400 cm with three tensiometers installed at 1-, 3-, and 5-cm depths was carried out on the Hanford sandy loam. This latter experiment was used to investigate the soil water pressure head and soil water content distribution with depth as a function of time. The duration of each pressure step ranged from near 6 h at the beginning of the experiment to 36 h at the end. Pressures

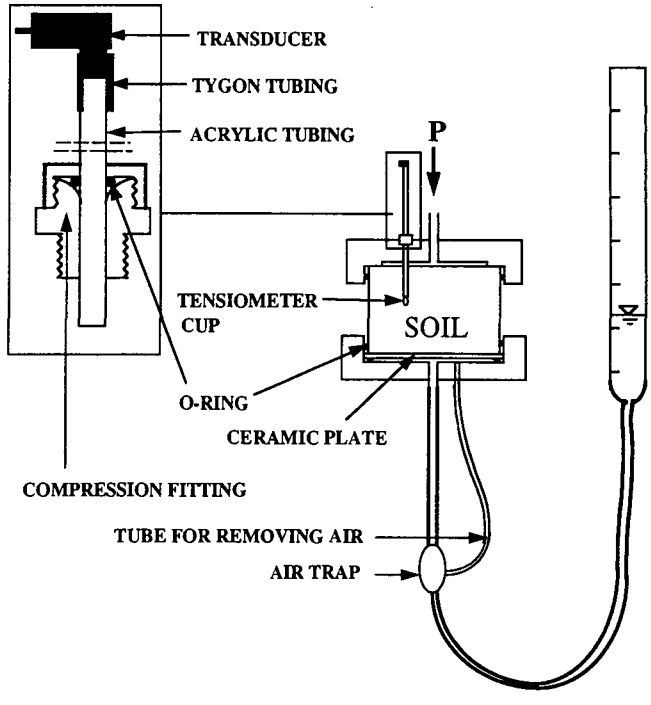

Fig. 1. A Schematic representation of the modified Tempe pressure cell for the multistep experiments.

were changed when outflow rate decreased to 0.05 mL h^{-1}, which corresponds to the beginning of the third stage of the outflow curve (Passioura, 1976). Cumulative outflow volume and soil water pressure head were measured as a function of time. Pressure head readings were recorded automatically at 1-min intervals for the full duration of the experiment. From experience, it was found that pressure head readings taken at times corresponding to 3-mL outflow increments during high flow rates, and 1-mL increments during low flow rates, were appropriate for both computer optimization and direct estimation of $K(\theta)$. At the end of the experiment, the soil columns were removed from the cells and weighed, over dried at 105°C for 24 h, and weighed again to determine the volumetric water content. This water content was then used together with the cumulative outflow volume and the volume outflow during the initial equilibration (−30 cm) to calculate the saturated and initial water contents.

The use of Eq. [1] and [3] in the inverse solution of the Richards equation implies that the optimization of the parameters α, n, θ_r, and K_s will yield a numerical solution that matches experimental data. The parameters α, n, θ_r, and K_s were optimized simultaneously by numerical inversion using the modified MULSTP code (MLSTPM) with cumulative outflow and soil water pressure head data in the objective function. A weighting scheme similar to that of Kool and Parker (1987) was used to combine auxiliary variables in one objective function. The saturated hydraulic conductivities of the ceramic

Table 1. Particle-size analyses and densities of investigated soils.

Soil	Sand	Silt	Clay	Bulk density
	%			g cm^{-3}
Yolo silt loam	23.0	55.5	22.5	1.17
Panoche loam	37.5	42.5	20.0	1.22
Hanford sandy loam	65.0	24.0	11.0	1.45
Oso Flaco fine sand	100.0	0.0	0.0	1.53

plates and θ_s were considered to be fixed. Saturated hydraulic conductivity of ceramic plates were determined from cumulative outflow volume for a Tempe cell filled with water when subjected to an arbitrarily chosen pneumatic pressure head of 400 cm. The calculated saturated conductivities of the plate were also used for the direct calculation of the unsaturated hydraulic conductivities of the four soils investigated. Additional information on the experimental procedure can be found in Eching and Hopmans (1993).

Direct $K(\theta)$ Method

Cumulative volume outflow and soil water pressure head data from the outflow experiments were used to compute $K(\theta)$ data, independent from the optimization method. When water drains from a short soil core through a porous plate of relatively high resistance, the hydraulic gradients in the soil are generally small (Ahuja and El-Swaify, 1976). Soil water pressure head at the soil–porous plate interface at any given time can be derived from the saturated hydraulic conductivity of the porous plate, the soil water pressure head maintained beneath the plate, and the water flux derived from outflow data (Ahuja, 1973). For a vertical column, steady flux through the porous plate is described by the Darcy equation:

$$q = -K_p\left(\frac{H_b - H_i}{d}\right) \quad [4]$$

where H_i is the total soil water head (cm) at the soil–plate interface, d is the thickness of the plate (cm), K_p is the saturated hydraulic conductivity of the plate (cm h^{-1}), q is the water flux (cm h^{-1}) calculated from cumulative outflow volume as a function of time, and H_b is the constant total soil water head at the bottom of the plate. With $z = 0$ defined at the soil surface, and downward flow direction considered positive, the total soil water head at the soil–plate interface is given by

$$H_i = H_b + \frac{d}{K_p}q \quad [5]$$

where it is assumed that, although the experiment is transient, the total head difference for the time interval during which q is measured is an arithmetic mean of the difference at the beginning and end of the interval.

To calculate the hydraulic conductivity of the soil, only one additional measurement of soil water pressure head within the soil core is needed. For that we used the pressure head measured at the center of the soil core. Analyses of pressure head distributions in the outflow experiment of the Hanford sandy loam with three tensiometers, as well as numerically generated data for the Panoche soil, showed that the total head at the soil surface and at 3-cm depth were the same within experimental error. The total head at the soil surface together with the calculated total head at the soil–plate interface were used to calculate the average head gradient in the core (Ahuja and El-Swaify, 1976). The corresponding average flux is assumed equal to the arithmetic mean of the fluxes at the two ends of the core, which is one-half of the value of outflow flux since a zero flux is maintained at the top of the soil core. For small time intervals, the average flux q is assumed to approximate steady-state flow. Hence, $K(\theta)$ is calculated using Darcy's equation:

$$K = -\frac{q}{\Delta H} \quad [6]$$

where ΔH is the average total head gradient in the core. Unlike the study presented by Ahuja and El-Swaify (1976) where the pressure gradient was imposed by a one-step change in the boundary condition, our study involved multiple step changes as described above. The column average θ value corresponding with each K value was computed from θ_s and the difference in cumulative outflow volume between the beginning and end of the considered time interval.

Evaporation Method

A detailed theoretical analysis of the evaporation method used has been presented by Wendroth et al. (1993). The Panoche loam used in the evaporation experiment had the same bulk density as the one used for the outflow experiments. The evaporation experiment was also carried out in the constant-temperature room at 20°C. In this study, a 6-cm-long packed soil column was placed on a porous plate, saturated from the bottom, and then placed on a plastic sheet. Tensiometer–transducer systems similar to the one used in the multistep outflow method were installed horizontally at 1-, 3-, and 5-cm depths, with each tensiometer representing the center of a compartment for a total of three. The transducers were connected to a datalogger with detachable wires.

Before initiation of evaporation, the sample was allowed to reach hydraulic equilibrium. After equilibrium, pressure head readings were taken, transducer wires were disconnected, and the soil sample was weighed. Evaporation was then initiated by blowing air across the soil surface with a fan. Soil water pressure head readings and the weight of the soil sample were taken at selected time intervals until the average pressure head gradient in the soil reached approximately 3.0 m m^{-1}. The fan was removed and the soil surface covered to allow the soil column to reach a new equilibrium. Thereafter, the cover was removed and evaporation was allowed to continue without the fan. The experiment was stopped when the soil water pressure head at the 1-cm depth was below −650 cm. The average soil water content at the end of the experiment was determined by oven drying at 105 °C. Using initial estimates for the parameters of Eq. [1], water contents and water storage values were calculated from tensiometer readings for each compartment at the selected time intervals. Total predicted water storage was compared with the measured water storage in the column, obtained by weighing the soil column at corresponding times. The difference between predicted and measured water storage was redistributed equally between the three compartments. Using the new water content and measured soil water pressure head values, Eq. [1] was fitted to obtain new parameters. This iterative estimation procedure (Wind, 1968) was repeated until the changes of estimated water content values between iterations were <0.0001 m^3 m^{-3}.

The average water flux between tensiometers located at 1- and 5-cm depths is estimated by (Wendroth et al., 1993)

$$q = \frac{1}{2\Delta t}\left(-\int_6^5 \Delta\theta\, dz - \int_6^1 \Delta\theta\, dz\right) \quad [7]$$

where the first integral denotes volume of water per unit area flowing into, and the second integral the volume per unit area flowing out of the compartment bounded by the 1- and 5-cm depths. Equation [7] can be approximated by following a quasi-stationary approach (Wendroth et al., 1993) assuming linearly increasing water content changes with decreasing soil depth for a specific time interval. The change in water storage is calculated as described above.

The average pressure head gradient for a particular time interval (Δt) is determined from the arithmetic mean of the pressure head gradients at the beginning and the end of the interval. The hydraulic conductivity is subsequently calculated by (Wendroth et al., 1993)

$$K = -\frac{q}{\frac{dh}{dz}\Big|_5^1 - 1} \quad [8]$$

The h corresponding to this K is calculated from the average h at the 1- and 5-cm depths at the beginning and end of the time interval considered. Further analysis (results not shown) considering the pressure head readings at 3-cm depth in addition to those at 1 and 5 cm showed that there were no apparent differences in the $K(h)$ functions separately calculated for the compartments 1 to 3 cm, 3 to 5 cm, or as presented here for the compartment between 1 and 5 cm.

Hydraulic conductivity was calculated according to Eq. [8]. Due to the uncertainty in the hydraulic gradient determination at the beginning of evaporation, hydraulic conductivity values calculated from gradients <0.2 m m^{-1} were discarded. The RETC code (van Genuchten et al., 1991) was used to optimize the hydraulic parameters θ_r, α, n and K_s simultaneously using the final soil water pressure heads obtained after the iterative process and measured $K(h)$ data. The RETC code was used since the MLSTPM method also optimizes $\theta(h)$ and $K(\theta)$ simultaneously. The $\theta(h)$ and measured $K(h)$ data and those obtained using the parameters from RETC where then compared with those obtained by MLSTPM optimization.

Infiltration Experiment

The infiltration experiment was carried out in a vertical column of air-dry Panoche loam soil (water content 0.022 m^3 m^{-3}) packed to the same bulk density as in the other experiments. The acrylic column was 18 cm long and circular in cross section with an inside diameter of 6.9 cm. Infiltration rate and cumulative infiltration were measured as a function of time, and soil water pressure head was measured continuously at depths of 3, 5.5, 8, 10.5, and 13 cm using the tensiometer–pressure transducer system described above. Tensiometers were installed just before the wetting front reached the measurement depth. Breather holes drilled 5 cm apart on opposite sides of the column allowed air escape during the experiment.

Water was applied at the surface of the soil through a fine mesh nylon membrane (Soil Moisture Systems, Tucson, AZ) maintained at a constant pressure head of −35 cm. The quantity of water entering the soil was measured with a Mariotte burette (0.2-mL accuracy). The position of the well-defined wetting front was monitored visually and from changing soil water pressure head values at the various tensiometer locations. The bottom of the column was open to the atmosphere. To eliminate the possible influence of the lower boundary condition on the infiltration process, the experiment was terminated when the wetting front reached 15.5-cm depth.

Cumulative infiltration, infiltration rate, wetting front position, and soil water pressure head as a function of depth and time were compared with results from a simulation model (J.W. Hopmans, 1988 unpublished data). The model, a fully implicit one-dimensional water flow model, solves the Richards equation numerically with the soil hydraulic functions represented by the van Genuchten functions. Soil water pressure head is the variable to be solved for in space and time. Grid spacing is 5 mm, time step is controlled by mass balance. The boundary conditions in the numerical simulation were set identical to those of the infiltration experiment with an upper pressure head boundary condition of −35 cm and lower pressure head boundary condition of −15 000 cm, corresponding to the 0.022 m^3 m^{-3} initial water content. The parameters of the soil hydraulic functions (Eq. [1] and [2]) and K_s were optimized by inverse solution of a step-wise sorption experiment using MLSTPM, with the values of n and θ_r assumed equal to those of the draining curve (Table 2), and θ_s equal to the water content at the end of the sorption experiment. The values of α, K_s, and θ_s were 0.0453 cm^{-1}, 120 cm d^{-1}, and 0.48 m^3 m^{-3}, respectively. This K_s value was close to the 128 cm d^{-1} value independently measured from steady-state saturated flow across the 18-cm column.

RESULTS AND DISCUSSION

Final parameter values and associated statistics obtained from the inversion of data of the multistep pressure experiment are presented in Table 2. The parameters in Table 2 are from Eching and Hopmans (1993) except those for the Panoche loam and the Hanford sandy loam that were obtained by using different initial parameter values. The inversion was carried out three times for each experiment, with the second and third initial parameter values generated automatically by the program. Results presented in Table 2 are those for a combination of highest correlation coefficient, r^2, and smallest sums of squares (SSQ) between observed and simulated data. High r^2 and low SSQ indicate a good correlation between the observed and fitted data. Our approach to testing for uniqueness was heuristic. Optimization of the hydraulic parameters was carried out three times, each time with different initial estimates of the parameter values. If convergence to the same final parameter values occurred for each of the three optimizations, we considered the solution unique. This approach is illustrated in Table 2 where coefficients of variation (CV) for the final parameter values are presented. The CV values are low for all parameters except for the θ_r and K_s of the Oso Flaco sand. These overall low CV values show that the multistep method results in unique solutions under our experimental conditions. Also presented in Table 2 are standard

Table 2. Final parameter values and statistics for the soils studied.

Parameter	Final estimate	CV
		%
	Yolo silt loam	
α, cm^{-1}	0.0367 ± 0.002†	0.04
n	1.572 ± 0.0245	0.00
θ_r, m^3 m^{-3}	0.161 ± 0.0098	0.00
K_{sat} (cm h^{-1})	5.876 ± 0.950	0.18
θ_s, (m^3 m^{-3})‡	0.552	
	Panoche loam	
α	0.0261 ± 0.0014	0.18
n	1.441 ± 0.0178	0.01
θ_r	0.0578 ± 0.0117	0.08
K_{sat}	1.954 ± 0.261	0.17
θ_s	0.50	
	Hanford sandy loam	
α	0.0094 ± 0.007	0.97
n	1.632 ± 0.0339	0.07
θ_r	0.010 ± 0.0168	0.14
K_{sat}	1.009 ± 0.174	2.25
θ_s	0.42	
	Oso Flaco fine sand	
α	0.0226 ± 0.0001	0.07
n	7.339 ± 0.2734	0.82
θ_r	0.032 ± 0.0054	5.48
K_{sat}	2.214 ± 0.331	3.42
θ_s	0.378	

† Standard error associated with the parameter.
‡ θ_s fixed in all the optimizations of four soils.

errors of estimation to indicate the measure of uncertainty associated with the estimated parameters. Soil water retention curves calculated using the final parameter values of Table 2 are shown in Fig. 2. Although estimation of $\theta(h)$ curves was not the main objective of this study, we present these curves since they are used to estimate soil water content associated with the optimized unsaturated hydraulic conductivities. The soil water retention curve obtained from optimization of sorption data for the Panoche soil is presented in Fig. 2b.

The direct calculation of $K(\theta)$ is based on the assumption that the soil water pressure head varies linearly with depth. Figure 3 shows simulated pressure head profiles for the Panoche loam and the Oso Flaco fine sand at selected times. Pressure head values measured with tensiometers at three depths in the Hanford soil column showed a distribution similar to that simulated for the Panoche soil. The simulated pressure head profiles for the Panoche soil (Fig. 3a) at 0.167, 0.334, and 0.303 h after pressure head step changes to 40, 80 and 100 cm, respectively, are linear. The remaining pressure head step changes, however, cause nonlinear distributions immediately after the change in the boundary condition. However, after approximately 1 h following these pressure changes, the head distribution becomes approximately linear. Nonlinearity at the beginning of each of these step changes increases with the magnitude of change relative to the previous pressure step. For example, as seen in Fig. 3a, the nonlinearity 0.866 h after the 700-cm step change is greater than that at 0.784 h after the 400-cm step. Moreover, the degree of nonlinearity as well as the pressure head step at which it occurs is soil dependent. The simulated pressure head profiles for the Oso Flaco sand (Fig. 3b) also show a linear distribution for the 40- and 60-cm pressure head steps. During the 40-cm step, the pressure head at the soil surface is significantly smaller than at 3-cm depth for the Oso Flaco sand column. In this range of saturation, the conductivity of the ceramic plate is impeding drainage. Consequently, the gradient across the soil column is small. Nonlinear pressure head distribution starts at the beginning of the 80-cm step for the Oso Flaco sand.

In view of the fact that Eching and Hopmans (1993) obtained excellent descriptions of $\theta(h)$ with van Genuchten's (1980) analytical expressions, we assumed that the expressions also adequately describe $K(\theta)$ for the same soils considered in this study. The solid lines in Fig. 4 show the optimized unsaturated hydraulic conductivity curves for all four soils estimated from the multistep outflow method with simultaneously measured soil water pressure head data. Directly measured hydraulic conductivity data using the modified method of Ahuja and El-Swaify (1976) are also shown in Fig. 4. The $K(\theta)$ values calculated from each of the pressure steps are also represented. The water content values in these figures were calculated from θ_s and cumulative outflow volume. Since experiments were started at -30 cm, measured $K(\theta)$ values near saturation are missing. The agreement between the optimized conductivity curves and measured conductivity data in Fig. 4 is excellent for Yolo silt loam (Fig. 4a) and Panoche loam (Fig. 4b); Hanford sandy loam shows good agreement (Fig. 4c). Oso Flaco fine sand (Fig. 4d) shows significantly lower measured than

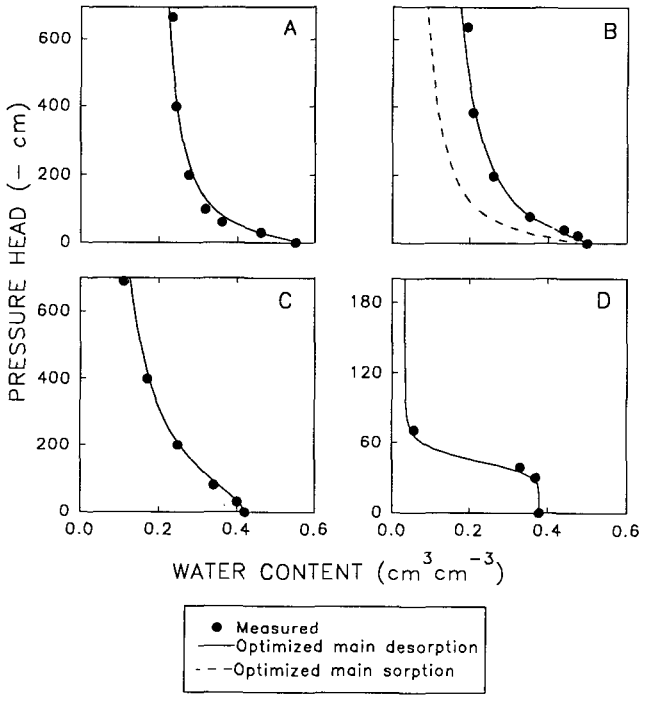

Fig. 2. Soil water retention curves for (A) Yolo silt loam, (B) Panoche loam, (C) Hanford sandy loam, and (D) Oso Flaco fine sand.

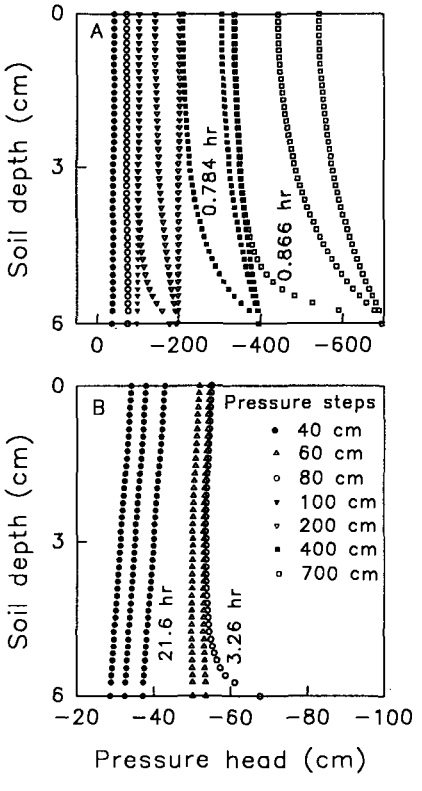

Fig. 3. Simulated soil water pressure head profiles at selected times for (A) Panoche loam and (B) Oso Flaco fine sand.

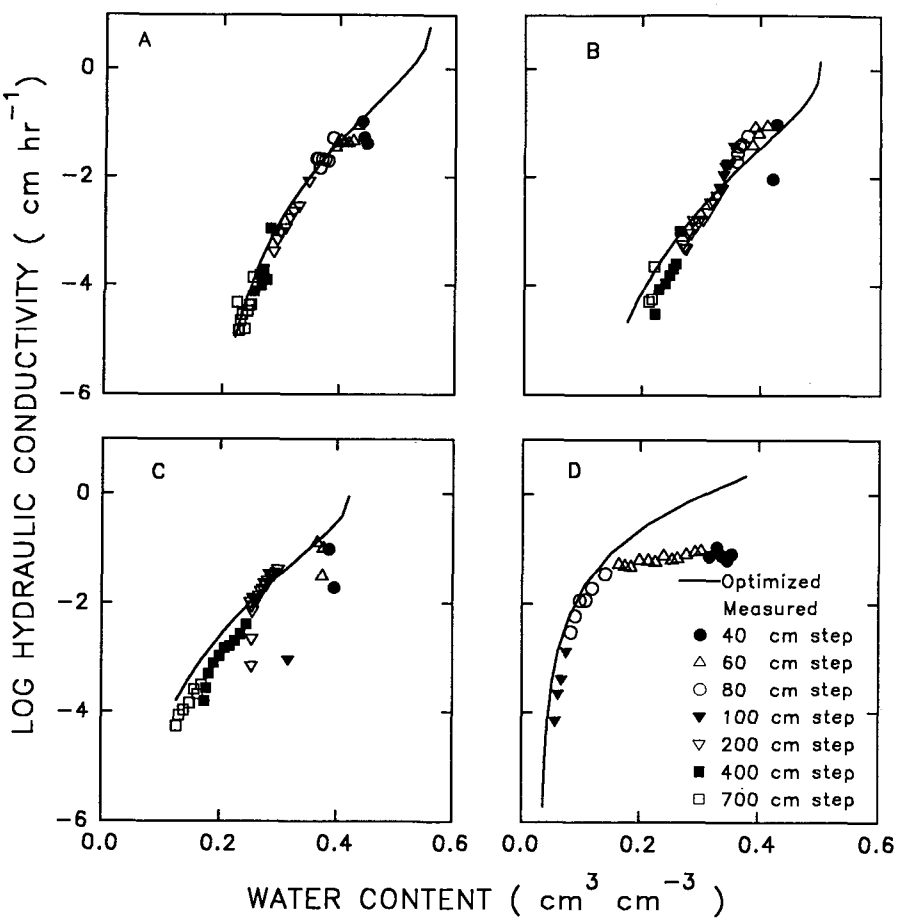

Fig. 4. Hydraulic conductivity curves for (A) Yolo silt loam, (B) Panoche loam, (C) Hanford sandy loam, and (D) Oso Flaco fine sand.

optimized data in the wet range, while the agreement is excellent in the dry range.

As shown in Fig. 3b, the simulated pressure head at the surface of the Oso Flaco soil column is significantly smaller than that at 3-cm depth for the 40- and 60-cm pressure head steps. Consequently, the average gradients estimated from extrapolation of measured soil water pressure heads at 3 cm to the soil surface are greater than the actual gradient in the column. Since the pressure head gradient in the wet range is small, an error in the gradient may cause relatively large errors in the calculated unsaturated hydraulic conductivity. The slow decrease of measured unsaturated hydraulic conductivity near saturation is attributed to the small changes in drainage rate and pressure head gradient (Fig. 3) during the 40- and 60-cm pressure head steps, with the near-constant drainage rate caused by the low conductivity of the porous plate relative to that of the sand in that pressure range (Hopmans et al., 1992). The measured conductivity data below the optimized curves at the beginning of the 40- and 60-cm steps for the Hanford sandy loam (Fig. 4c) and at the beginning of the 40-cm step for the Yolo silt loam (Fig. 4a) and the Panoche loam (Fig. 4b) is also a result of a violation of the assumptions involved in the calculation of the average gradient. The low measured conductivity data at the end of the 100- and 200-cm pressure steps for the Hanford sandy loam (Fig. 4c) are caused by violation of the steady-state flow assumption. A considerable amount of time was needed for a significant volume of water to drain from the soil, with the drainage rate decreasing with time. Consequently, fluxes calculated from the volume of water are skewed to lower values, resulting in an underestimation of the corresponding hydraulic conductivity.

Our measurement technique appears unreliable in the wet range for Oso Flaco fine sand. The underestimation in Fig. 4d is primarily caused by violation of the assumptions in the calculations of the unsaturated hydraulic conductivity. While the optimized retention curve for the Oso Flaco sand agrees well with the measured data (Fig. 2), we have not been able to test the accuracy of the optimized conductivity curve. We believe, however, that the optimized unsaturated hydraulic conductivity curve for the Oso Flaco sand is realistic because the conductivity of the plate is taken into account in the optimization. The results in Fig. 4d indicate that, for the Oso Flaco soil, the pressure head should be measured at the soil surface rather than at 3-cm depth in order to more accurately determine the pressure head gradient.

A comparison of the parameter estimation method with the evaporation method for the Panoche loam is presented in Fig. 5. Two $\theta(h)$ curves estimated from the evaporation method are presented in Fig. 5a. The first curve (dashed line) was obtained by using the retention data of the evaporation experiment obtained with the iterative technique. The second curve (dotted line) was subsequently deter-

mined from a simultaneous fit of the same $\theta(h)$ data and the measured $K(h)$ using RETC. We include this curve, since the MSLTPM method (solid lines) also optimizes the parameters of $\theta(h)$ and $K(\theta)$ simultaneously. The two $\theta(h)$ curves derived from the evaporation method agree well with the MLSTPM curve. Deviations increase toward the dry end, however, possibly caused by experimental error or due to different soil columns used for the two methodologies. The measured data points and the RETC curve in Fig. 5c agree well, except for a slight deviation in the dry end. This is caused by the relatively few water retention data points in the dry range for the parameter fitting of $\theta(h)$ and $K(\theta)$ with RETC. Deviations between the measured $K(h)$ data and optimized MLSTPM curve occur in both the dry and wet range. Differences in the dry range are similar to the differences between the two $\theta(h)$ curves in this range. The differences between the measured data and the MLSTPM results near saturation are probably due to slight differences in the macropore space of the soil columns used.

Overall, we believe that the multistep parameter estimation method with simultaneously measured cumulative outflow and soil water pressure head data gave adequate unsaturated hydraulic conductivity functions in view of the excellent agreement with the directly measured $K(h)$ data for three soils with different textures. Also the independently measured data using the evaporation method for the Panoche loam agreed well with the multistep method. The optimized K_s values have no physical meaning and are fitting parameters only. Since experiments were started with unsaturated soil samples, neither of the presented methodologies is accurate in the range wetter than −30 cm (van Dam et al., 1992). In the dry range, the results of the optimization can be extended by including steady-state retention points from pressure plate data in the objective function.

Comparisons of measured with simulated infiltration rate, cumulative infiltration, and depth distribution of soil water pressure head as a function of time for Panoche loam are presented in Fig. 6. We used the soil hydraulic

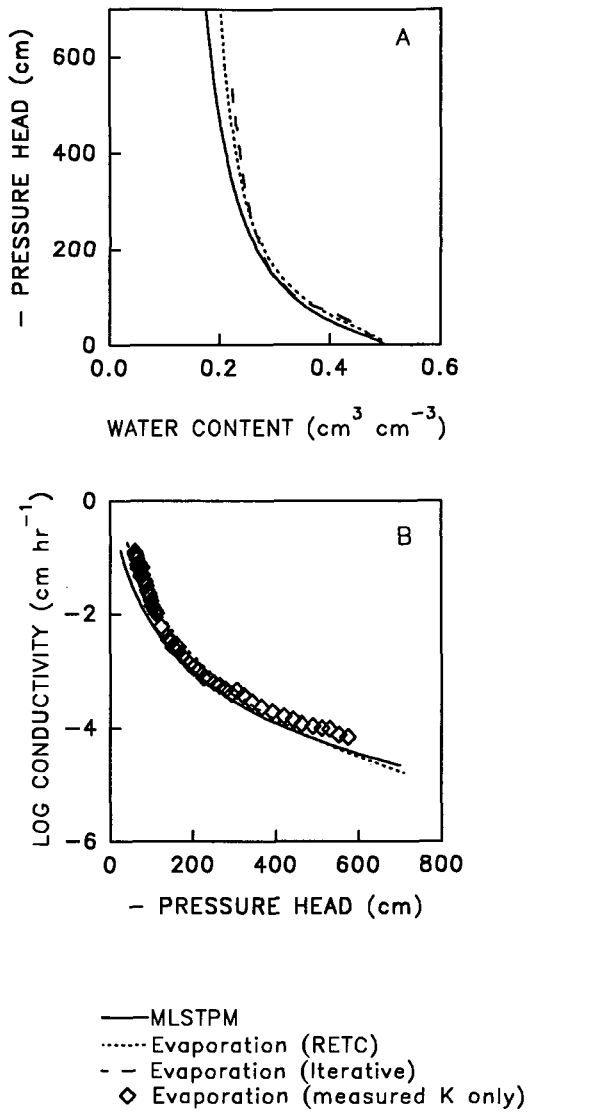

Fig. 5. (A) Soil water retention curves and (B) hydraulic conductivity curves for Panoche loam from MLSTPM and evaporation methods.

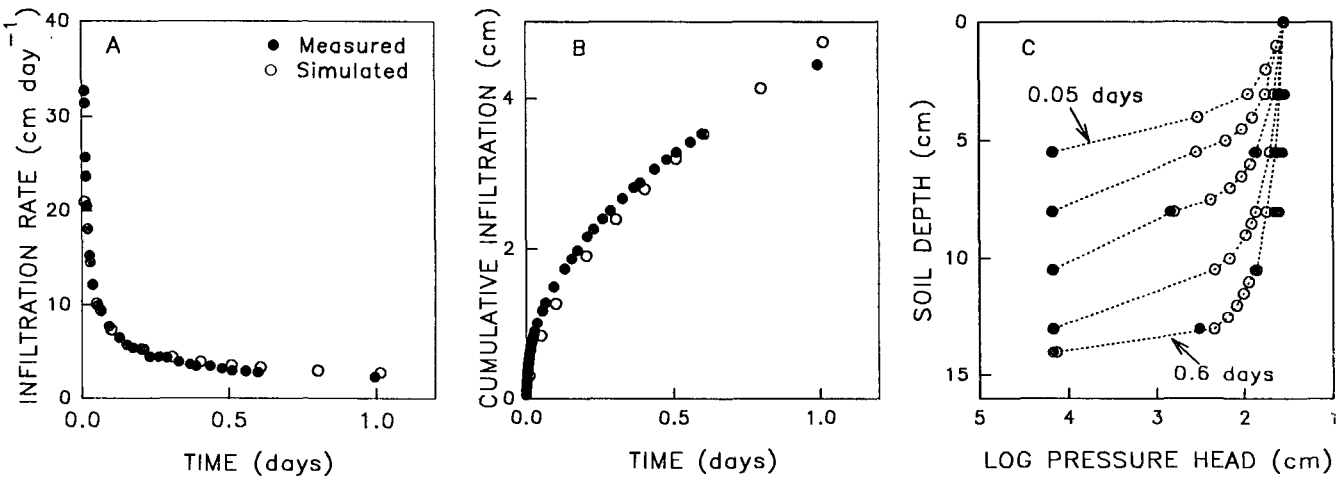

Fig. 6. Experimental and simulated (A) infiltration rate, (B) cumulative infiltration, and (C) pressure head profile for Panoche loam.

functions optimized from the multistep outflow (n and θ_r) and sorption (α, K_s, and θ_s) experiments as input to the water flow model. Soil hydraulic functions were optimized for a sorption experiment since infiltration into a dry soil is a wetting process. Since the multistep outflow experiment does not necessarily describe the soil hydraulic conductivity function well near saturation, we choose an upper boundary condition of -35 cm in the infiltration experiment. The simulated infiltration rate (Fig. 6a) and cumulative infiltration (Fig. 6b) agree well with the experimental data. Figure 6c presents a comparison between the simulated and experimental soil water pressure head distributions at selected times. Although the depth resolution is different for measurements and simulations, the overall agreement is excellent. Often, soil hydraulic functions are needed as input for numerical flow models; the selection of the method of determination of the hydraulic functions should then be based on the accuracy of numerical results. The good agreement between simulated and experimental infiltration suggests that the hydraulic functions, as determined from the inverse solution technique presented here, are accurate.

SUMMARY AND CONCLUSIONS

The inverse determination of unsaturated soil hydraulic conductivity functions from simultaneously measured transient cumulative outflow and soil water pressure heads was examined. We have confirmed the theoretical intuition (Toorman et al., 1992; van Dam et al., 1992) of using more auxiliary variables through laboratory experimentation. There is excellent agreement between experimental and simulated infiltration with the optimized soil hydraulic parameters as model inputs. Although the results and the analysis were restricted to pressurized multistep experiments, they are equally applicable to multistep suction experiments (Eching and Hopmans, 1993).

The general excellent agreement between MLSTPM curves and the directly measured hydraulic data for the Yolo, Panoche, and Hanford soils and the evaporation method for the Panoche soil leads us to conclude that our inverse solution technique yields realistic unsaturated hydraulic conductivity functions. We also found that the same experimental setup and optimization algorithm can be used to estimate the wetting soil hydraulic functions.

We emphasize that these methods are influenced strongly by a changing saturated hydraulic conductivity of the porous plate. Therefore, one should measure the saturated hydraulic conductivity of the porous plate before and after the experiment to ascertain that no changes in plate conductivity have occurred during the experiment. Plate conductivity may change due to clogging by dirt or bacteria if untreated water is used. All soils used in this study were disturbed, thereby reducing the inherent variability present in undisturbed soil samples. The sensitivity of soil water pressure head measurements on the optimization results will be affected by soil variability. Although we recommend that a tensiometer be installed at or just below the soil surface when the direct measurement technique is used with coarse-textured soils, the influence of soil water pressure head measurement depth on the optimization needs to be investigated.

Optimized unsaturated hydraulic conductivity functions determined from soil columns do not necessarily represent in situ soil hydraulic functions. On the other hand, this laboratory method allows considerable flexibility in the choice of initial and boundary conditions. Moreover, considerable time is saved by carrying out transient experiments. Multistep outflow experiments under the experimental conditions in this study lasted 3 to 7 d; this duration could be shorter with different experimental conditions and varies with soil type. In our laboratory, outflow experiments are carried out for 40 soil samples simultaneously, thus making it suitable for characterizing numerous soil cores from a field.

Our heuristic approach to testing uniqueness of the optimized parameter values indicates that the problem of uniqueness is reduced if cumulative outflow volume and simultaneously measured soil water pressure head data are used in the objective function. Also based on the excellent comparison of independently measured $\theta(h)$ data with those optimized using the multistep outflow technique (Eching and Hopmans, 1993), we believe that our technique provides an excellent alternative for unsaturated hydraulic function measurements, especially if accurate soil hydraulic information for a large number of samples is needed across a relatively wide soil water pressure head range.

ACKNOWLEDGMENTS

Research supported by the U.S. Geological Survey, Department of the Interior, under USGS award no. 14-08-001-G1910. The views and conclusion contained in this document are those of the authors and should not be interpreted as necessarily representing the official policies, either expressed or implied, of the U.S. Government. Additional funding was provided by the University of California Salinity/Drainage Task force.

REFERENCES

Ahuja, L.R. 1973. A numerical and similarity analysis of infiltration into crusted soils. Water Resour. Res. 9:987–994.

Ahuja, L.R., and S.A. El-Swaify. 1976. Determining both water characteristic and hydraulic conductivity of a soil core at high water contents from a transient flow experiment. Soil Sci. 121: 198–205.

Arya, L.M., D.A. Farrell, and G.R. Blake. 1975. A field study of soil water depletion patterns in presence of growing soybean roots: I. Determination of hydraulic properties of the soil. Soil Sci. Soc. Am. Proc. 39:424–430.

Burdine, N.T. 1953. Relative permeability calculations from pore-size distribution data. Trans. Am. Inst. Min. Metall. Pet. Eng. 198: 7–77.

Childs, E.C., and N. Collis-George. 1950. The permeability of porous materials. Proc. R. Soc. London Ser. A 201:392–405.

Dane, J.H., and S. Hruska. 1983. In-situ determination of soil hydraulic properties during drainage. Soil Sci. Soc. Am. J. 47:619–624.

Dirksen, C. 1979. Flux-controlled sorptivity measurement to determine soil hydraulic property. Soil Sci. Soc. Am. J. 43:827–834.

Eching, S.O., and J.W. Hopmans. 1993. Optimization of hydraulic functions from transient outflow and soil water pressure data. Soil Sci. Soc. Am. J. 57:1167–1175.

Flocker, W.J., M. Yamaguchi, and D.R. Nielsen. 1968. Capillary conductivity and soil water diffusivity values from vertical soil columns. Agron. J. 60:605–610.

Gardner, W.R. 1956. Calculation of capillary conductivity from pressure outflow data. Soil Sci. Soc. Am. Proc. 20:317–320.

Hopmans, J.W., T. Vogel, and P.D. Koblik. 1992. X-ray tomography of soil water distribution in one-step outflow experiments. Soil Sci. Soc. Am. J. 56:355–362.

Klute, A., and C. Dirksen. 1986. Conductivities and diffusivities of unsaturated soils. p. 687–734. *In* A. Klute (ed.) Methods of soil analysis. Part 1. 2nd ed. Agron. Monogr. 9. ASA and SSSA, Madison, WI.

Kool, J.B., and J.C. Parker. 1987. Estimating soil hydraulic properties from transient flow experiments: SFIT user's guide. Dep. of Soils and Environ. Sci., Virg. Polytech. Inst. and State Univ., Blacksburg.

Kool, J.B., and J.C. Parker. 1988. Analysis of the inverse problem for transient unsaturated flow. Water Resour. Res. 24:817–830.

Kool, J.B., J.C. Parker, and M.Th. van Genuchten. 1985. Determining soil hydraulic properties from one-step outflow experiments by parameter estimation. I: Theory and numerical studies. Soil Sci. Soc. Am. J. 49:1348–1354.

Kool, J.B., J.C. Parker, and M.Th. van Genuchten. 1987. Parameter estimation for unsaturated flow and transport models – A review. J. Hydrol. (Amsterdam) 91:255–293.

Mualem, Y. 1976. A new model for predicting the hydraulic conductivity of unsaturated porous media. Water Resour. Res. 12:513–522.

Nielsen, D.R., D. Kirkham, and E.R. Perrier. 1960. Soil capillary conductivity: Comparison of measured and calculated values. Soil Sci. Soc. Am. Proc. 24:157–160.

Passioura, J.B. 1976. Determining soil water diffusivities from one-step outflow experiments. Aust. J. Soil Res. 7:79–90.

Plagge, R., M. Renger, and C.H. Roth. 1990. A new laboratory method to quickly determine the unsaturated hydraulic conductivity of undisturbed soil cores within a wide range of textures. Z. Pflanzenernähr. Bodenkd. 153:39–45.

Russo, D., E. Bresler, U. Shani, and J.C. Parker. 1991. Analysis of infiltration events in relation to determining soil hydraulic properties by inverse problem methodology. Water Resour. Res. 27: 1361–1373.

Toorman, A.F., P.J. Wierenga, and R.G. Hills. 1992. Parameter estimation of hydraulic properties from one-step outflow data. Water Resour. Res. 28:3021–3028.

van Dam, J.C., J.N.M. Stricker, and P. Droogers. 1990. From one-step to multi-step determination of soil hydraulic functions by outflow experiments. Dep. of Water Resour. Rep. no. 7. Wageningen Agric. Univ., Wageningen, the Netherlands.

van Dam, J.C., J.N.M. Sticker, and P. Droogers. 1992. Inverse method for determining soil hydraulic functions from one-step outflow experiments. Soil Sci. Soc. Am. J. 56:1042–1050.

van Genuchten, M.Th. 1980. A closed-form equation for predicting the hydraulic conductivity of unsaturated soils. Soil Sci. Soc. Am. J. 44:892–898.

van Genuchten, M.Th., F.J. Leij, and S.R. Yates. 1991. The RETC code for quantifying the hydraulic functions of unsaturated soils. USAEPA Rep. 600/2-91/065. U.S. Gov. Print. Office, Washington, DC.

Watson, K.K. 1967. The measurement of the hydraulic conductivity of unsaturated porous materials utilizing a zone of entrapped air. Soil Sci. Soc. Am. Proc. 31:716–720.

Wendroth, O., W. Ehlers, J.W. Hopmans, H. Kage, J. Halbertsma, and J.H.M. Wösten. 1993. Reevaluation of the evaporation method for determining hydraulic functions in unsaturated soils. Soil Sci. Soc. Am. J. 57:1436–1443.

Wind, G.P. 1968. Capillary conductivity data estimated by a simple method. p. 181–191. *In* P.E. Rytema and H. Wassink (ed.) Water in the unsaturated zone. Proc. Wageningen Symp. Vol. 1. IASAH, Gentbrugge, the Netherlands. June 1966.

Yeh, W.W.-G. 1986. Review of parameter identification procedures in groundwater hydrology: The inverse problem. Water Resour. Res. 22:95–108.